DISLOCATION DYNAMICS OF YIELDING AND FRACTURE

by

G. T. Hahn, C. N. Reid, and A. Gilbert
Battelle Memorial Institute

INTRODUCTION

Many recent observations on the submicroscopic scale have revealed the presence of both regular and irregular arrangements of dislocations in crystals. Such submicroscopic features fall under the general heading of substructure. Of these dislocations many are immobile, while the rest are free to move under the action of an applied stress. Study of the mobile dislocations has led to the development of a treatment which may be termed Dislocation Dynamics, the object of which is to predict deformation behavior from a knowledge of dislocation parameters.

The dislocation dynamics practiced in the 1950's accepted that the generation of mobile dislocations is difficult but their movement through the lattice is easy. Consequently, the processes for generating free dislocations--nucleation, unpinning, or multiplication--were regarded as rate controlling. More recently, however, the opposite view has gained support. This has come about largely through the work of Johnston and Gilman[1] at the G. E. Research Laboratory, who made three important contributions. First they showed by direct measurement that dislocations do not accelerate freely in lithium-fluoride crystals, but travel with a well defined velocity. Secondly, they formulated a concise statement of the dislocation dynamics of flow in terms of the velocity of the dislocations and the number moving. Finally, they used

this expression to calculate from the basic dislocation parameters a stress-strain curve of lithium-fluoride crystals. Since then, dislocation velocities have been measured in a number of other materials, including Fe-3.25Si crystals[2,3], silicon[4], germanium[4,5], and tungsten[6], and the treatment extended to describe other features of yielding such as the strain rate dependence of the yield stress, the delay time for yielding, and the Lüders' band.[7] These studies tend to identify the dislocation velocity, rather than the rate of generation, as the more important variable.

Dislocation Velocity

Johnston and Gilman measured dislocation velocity in the following way. The surface of a crystal was indented to produce free dislocations, whose positions were revealed by etch-pitting. The crystal was then stressed for a known time and re-etched. The pitting technique was such that the old and new positions of the dislocations were distinguished. They found that the distance moved at any given stress was proportional to the time duration of the stress, and from this they calculated a mean velocity. This is not to say that the dislocation moved through the lattice with constant speed, as is shown schematically in Figure 1a. For example, evidence exists that dislocation movement on the atomistic scale proceeds discontinuously by thermal activation at a succession of barriers. The motion may therefore be looked upon as a repeated sequence of release and arrest, as shown in Figure 1b. Since only one segment of the dislocation may be stopped at any one time, Figure 1c may be a truer representation.

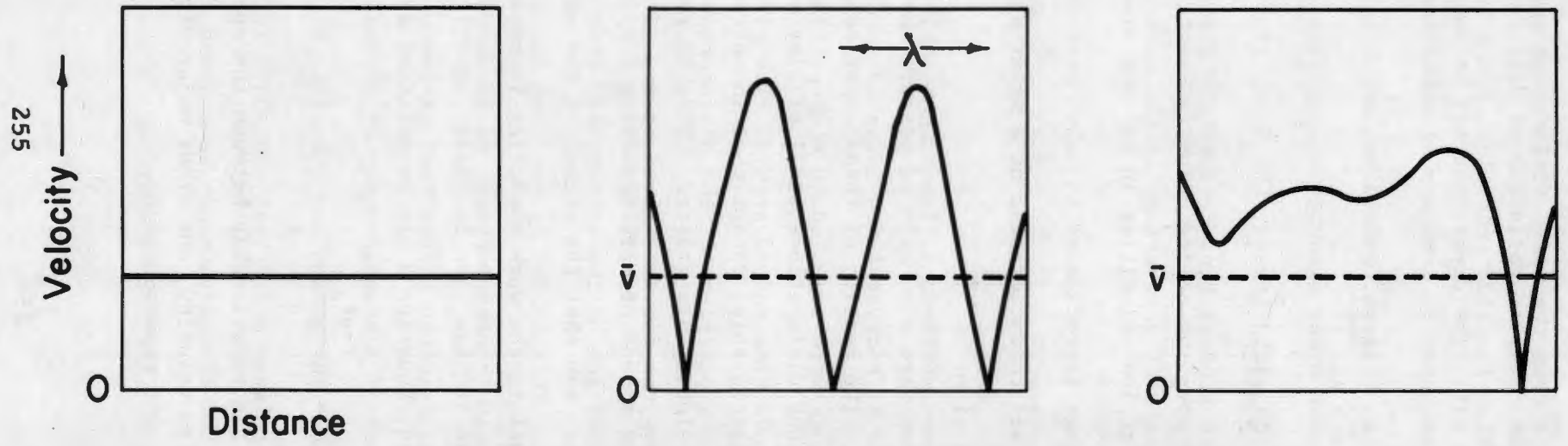

1a 1b 1c

FIGURE 1. SCHEMATIC ILLUSTRATION OF THE MOTION OF A DISLOCATION SEGMENT.

Figure 2a shows the observed variation of dislocation velocity, $\bar{v}$, with shear stress, τ, in LiF. The dependence may be described by the formulae:

$$\bar{v} = Ae^{\frac{-B(T)}{\tau}} , \qquad (1)$$

$$\bar{v} = \left\{\frac{\tau}{\tau_o}\right\}^m . \qquad (2)$$

Equation (1) applies to LiF over the entire velocity spectrum, whereas Equation (2) is applicable at low velocities in LiF and also over the more restricted velocity range investigated in other materials. The values assumed by m and τ_o are characteristic of a material, and Table 1 summarizes published values of m.

Johnston and Gilman were also able to measure the velocity in slightly deformed crystals. The results of these experiments, shown in Figure 2b, illustrate that the dislocations still display essentially the same velocity-stress relationship, except that the stresses associated with any given velocity are greater. This increase in stress corresponds closely with the amount of work-hardening displayed by the stress-strain curve. One may say that the effect of the applied stress is reduced by an amount equal to the work hardening increment, but more research must be done to see if this view is really justified. Assuming a linear work-hardening rate, Equation 2 can be modified as follows:

$$\bar{v} = \left\{\frac{\tau - q\epsilon_p}{\tau_o}\right\}^m \qquad (3)$$

Having described the relationship between the applied stress and the resultant dislocation velocity, one other major variable remains

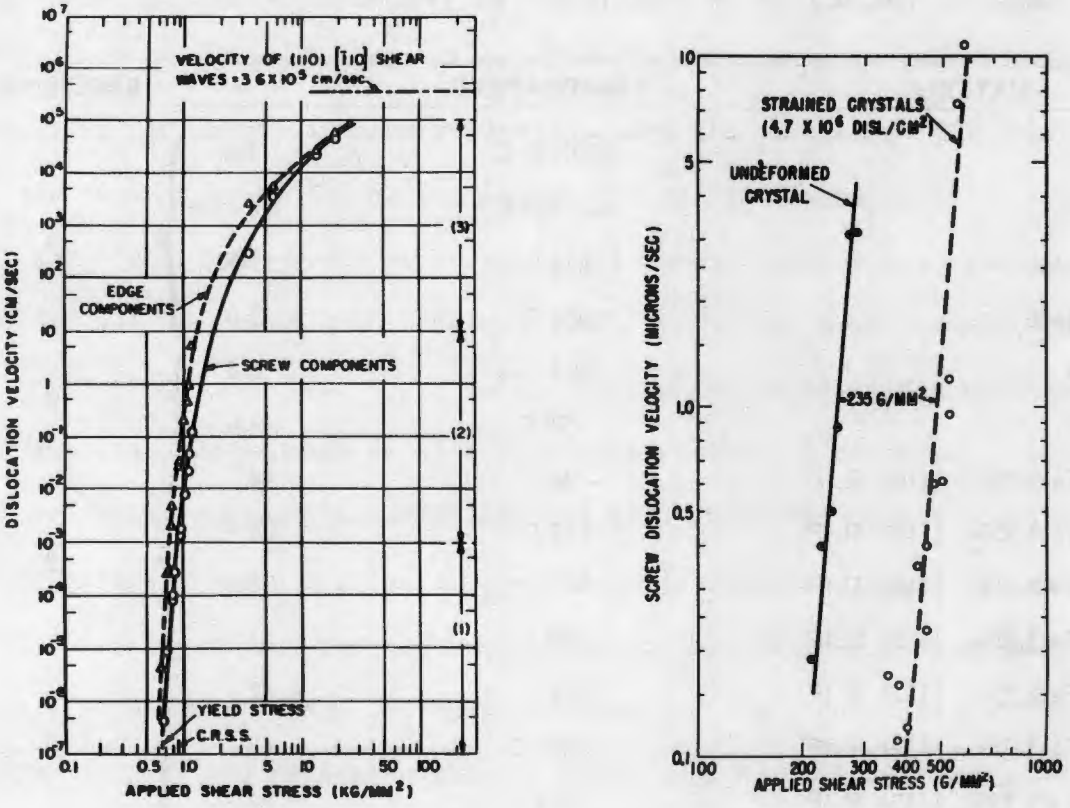

2a 2b

FIGURE 2. a. Variation of dislocation velocity with applied shear stress in LiF crystals[1].

b. Effect of strain on dislocation mobility in LiF[35].

TABLE 1. VALUES OF m PUBLISHED IN THE LITERATURE

MATERIAL	TEMPERATURE	m	REFERENCE
Si	600-900 C	1.4	4
Ge	420-700 C	1.4 - 1.9	
InSb	218 C	1.87	
GaSb	450 C	2.0	
W	R.T.	5.0	6
W	-196 C	14.0	
Fe-3.25Si, {110} SLIP	-196 C	44	2
Fe-3.25Si, {110} SLIP	-77 C	38	
Fe-3.25Si, {110} SLIP	R.T.	35	
Fe-3.25Si, {110} SLIP	100 C	41	
Fe-3.25Si, {112} SLIP	-77 C	42	3
Fe-3.25Si, {112} SLIP	-40 C	43	
Fe-3.25Si, {112} SLIP	R.T.	34	
LiF	R.T.	14.5 ± 2	1

before dislocation dynamics can be applied, namely the number of dislocations actually moving.

Dislocation Density

It is known that most annealed crystals possess a grown-in dislocation density of about 10^6 to 10^8 cm/cm^3. In certain cases, however, these dislocations are tightly bound by impurity atmospheres or precipitates, and when the crystal is stressed, these grown-in dislocations frequently do not move. Instead, mobile dislocations are produced either by heterogeneous nucleation or unpinning at points of high stress such as inclusion particles or discontinuities at the grain boundaries. Precipitate particles are particularly effective sites for nucleation. An example of this is presented in Figure 3, which shows dislocation loops produced by precipitate particles in unalloyed chromium, and revealed on the surface by etching. The dislocations produced in this way then move through the crystal and multiply rapidly, probably by the double cross-slip mechanism. As a result, the dislocation density increases rapidly as the material is deformed. The change in dislocation density with strain has now been studied in a number of materials by etch pitting and by transmission microscopy. Such studies, however, do not permit a distinction to be made between dislocations which are immobile and those which are able to move. The only experimental evidence currently in the literature concerning the fraction, f, which is mobile, is due to Patel and Chaudhuri.[4] They were able to infer the value of f in a few isolated cases involving small strains and report values in the range between 0.08 and 1. It is unlikely that f is a constant except perhaps in the early stages of yielding, and the formulation of f from experiment

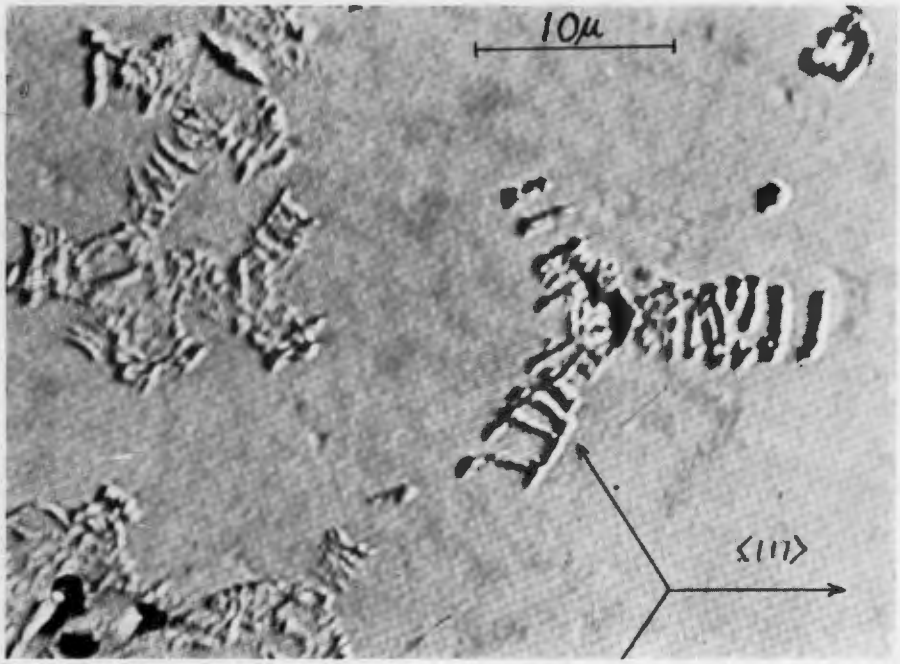

FIGURE 3. NUCLEATION OF DISLOCATIONS BY PRECIPITATE PARTICLES IN CHROMIUM[36].

or theory is a problem deserving of more attention. In the absence of such a formulation however, the assumption is made that the total density, ρ, is simply related to the mobile density, ρ'.

Typical examples of the rate of increase of total dislocation density with strain are presented in Figure 4, which shows results obtained at Battelle for a mild steel using transmission electron microscopy. The dislocation density increases from about 5×10^8 cm/cm^3 in the annealed material, to about 10^{10} after 10 per cent deformation. These experiments were carried out at three widely differing strain rates, about 10^{-5} per second, 10^{-2} per second, and 10^3 per second, a range of nearly eight orders of magnitude. The figure illustrates that the rate of multiplication in this material at least is relatively insensitive to strain rate. This is illustrated qualitatively in Figure 5, which shows examples of the transmission micrographs that were obtained at the three different strain rates. The main difference is that the dislocation segments tend to be more straight and parallel at the highest strain rate.

The experimentally measured dislocation densities can be described by an equation of the form:

$$\rho = \rho_o + C\epsilon_p^{\beta}, \qquad (4)$$

where ρ_o represents the initial dislocation density and C and β are multiplication parameters. Values of β are in the range 1/2 to 3/2, but are usually close to 1. This expression describes the total number of dislocations that have been generated and does not distinguish between

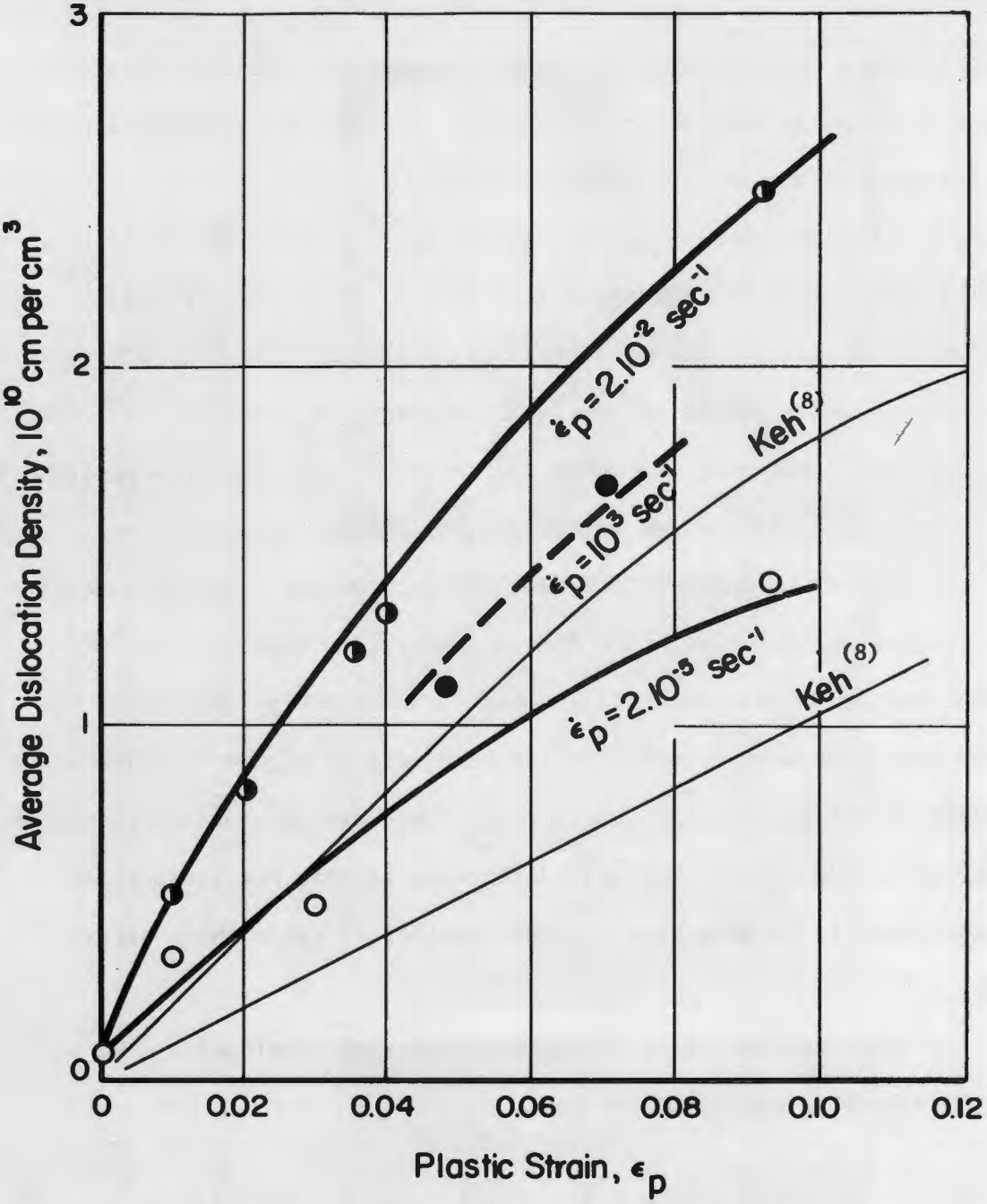

FIGURE 4. INCREASE OF DISLOCATION DENSITY WITH STRAIN IN MILD STEEL DEFORMED AT DIFFERENT RATES.

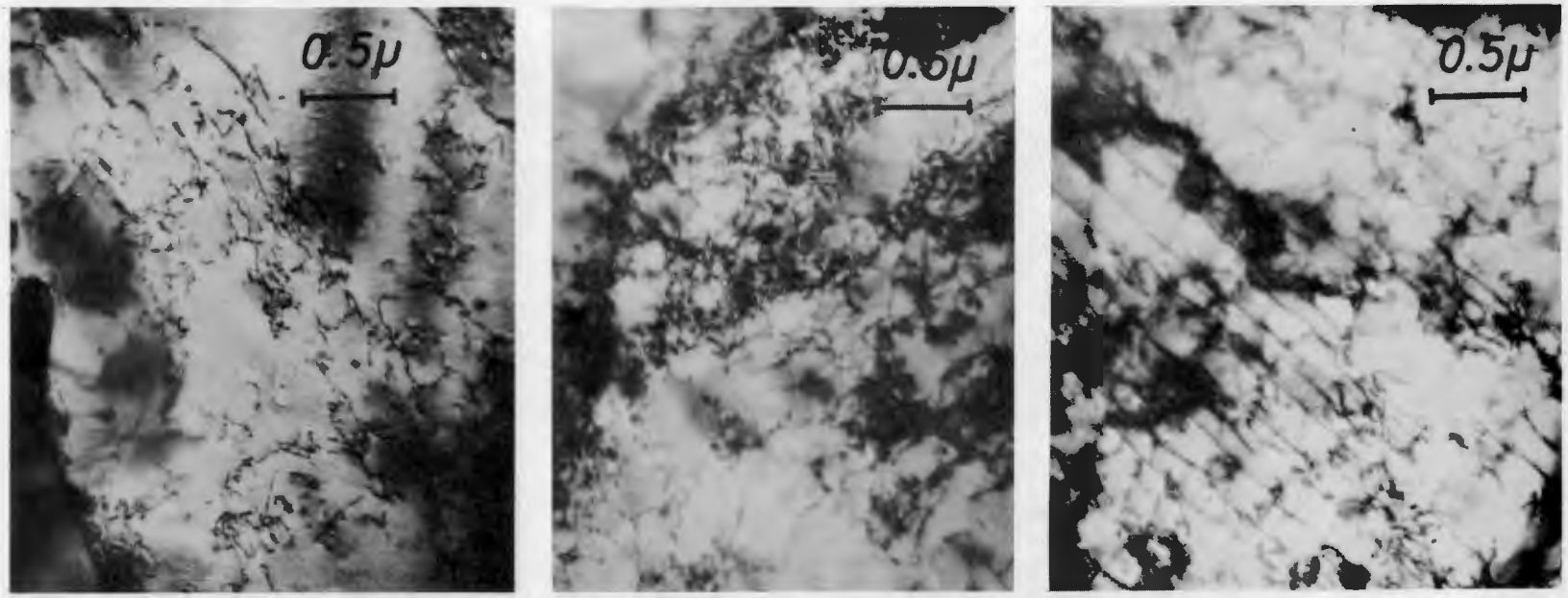

FIGURE 5. ELECTRON MICROGRAPHS OF THE SUBSTRUCTURES PRESENT IN MILD STEEL AFTER DEFORMATION AT VARIOUS STRAIN RATES, TO 3% STRAIN.

the ones that are still mobile and those that have become arrested. The relevant parameter is the mobile density, which can be described, at least in a very approximate way, by the equation,

$$\rho' = \rho_o' + fC\varepsilon_p \quad , \tag{5}$$

where ρ_o' represents the number of dislocations initially mobile and f the fraction of the dislocations subsequently generated that is mobile.

Table 2 summarizes available information regarding the value of the multiplication parameter, C. These values show that there are significant differences in the rate of multiplication. The results for copper, for example, show that multiplication is more rapid in polycrystalline samples than in single crystals. Consistent with this, Keh[8] investigated the rates of multiplication in iron of two grain sizes, and found the rate to be higher in the fine grained material.

Utilizing the above data, dislocation dynamics can now be applied to describe plastic flow in response to a variety of loading conditions.

DISLOCATION DYNAMICS

The new knowledge of the velocity of dislocations and their rate of multiplication is important in its own right. However, its significance was not fully appreciated until Johnston and Gilman formulated a concise statement of the dislocation dynamics of flow. They pointed out that the deformation accompanying the application of stress consists of an elastic and a plastic contribution. For instance, in a

TABLE 2 . VALUES OF THE DISLOCATION MULTIPLICATION PARAMETER $C = \left(\frac{d\rho}{d\epsilon}\right)_{\epsilon = 1\%}$ FOR A VARIETY OF MATERIALS

MATERIAL	S: SINGLE CRYSTAL P: POLYCRYSTALLINE	C $(CMS^2 \cdot PER\ CENT)^{-1}$
COPPER [10-12]	S P	$3\text{-}9 \times 10^6$ 5×10^8
LITHIUM FLUORIDE [1]	S	1×10^7
GERMANIUM [4,5,9]	S	$4\text{-}80 \times 10^6$
NIOBIUM [13]	P	4×10^9
TANTALUM [14]	P	1.7×10^{10}
MOLYBDENUM [15]	P	8×10^8
TUNGSTEN [6]	S	2×10^7
IRON [8]	P	1.5×10^9
MILD STEEL [16]	P	$2\text{-}4 \times 10^9$

constant strain rate test, the strain rate, $\dot{\epsilon}$, imposed by the machine must be matched by the sum of the elastic and plastic components, $\dot{\epsilon}_e$ and $\dot{\epsilon}_p$, of the strain rate in the specimen.

$$\dot{\epsilon} = \dot{\epsilon}_e + \dot{\epsilon}_p \tag{6}$$

The elastic contribution can be expressed in terms of the rate of stress application and a modulus, M, which reflects the stiffness of the test bar, grips, and supporting members. The plastic contribution is given by the equation[17]

$$\dot{\epsilon}_p = 0.5\ b\ \rho'\ \bar{v} \tag{7}$$

where b is the Burgers vector for slip, and 0.5 arises from geometrical considerations. Equation (6) may therefore be written

$$\dot{\epsilon} = \frac{1}{M}\frac{d\sigma}{dt} + 0.5\ b\ \rho'\ \bar{v} \tag{8}$$

where σ refers to tensile stress. Substituting in Equation (8) from Equations (3) and (5) yields

$$\dot{\epsilon} = \frac{1}{M}\frac{d\sigma}{dt} + 0.5\ b\ (\rho_o' + fC\epsilon_p)\ (\sigma - q\epsilon_p)^m\ (\sigma_o)^{-m} \tag{9}$$

the shear stresses, τ and τ_o from Equation (3), being replaced by the equivalent tensile stresses σ and σ_o. This differential equation may be solved to describe the stress-strain relationship for a single crystal.

The behavior of polycrystalline samples is complicated by

the variation of the resolved shear stress from grain to grain owing to the different grain orientations, the anisotropy of the modulus and the constraints imposed by neighboring grains. In principle at least, the deformation of polycrystalline samples can be described by a summation over all the grains of the aggregate. It should be noted that such parameters as ρ_o, f, c, and q may depend on grain size, a fact Conrad has used to derive the yield stress grain-size relation for steel.[18]

Application to Yielding

Johnston and Gilman first used the dislocation dynamics approach to calculate the stress-strain curve of lithium-fluoride crystals. When an empirical correction is made for the effect of work hardening, and plausible values adopted for f and ρ_o', the curve calculated from Equation (9) agrees very well with that determined experimentally.

More recently, Johnston[19] has solved the equation for simple tension with the aid of a computer for various values of the parameters m and ρ_o'. Figure 6 demonstrates the influence of ρ_o' on the shape of the stress-strain curve, all other parameters being kept constant. The effect of m is illustrated in Figure 7a. These calculations show that the initial yield drop is a general feature of small values of ρ_o' and small values of m. The predicted effect of ρ_o' (Figure 6) correlates well with the observed occurrence of a yield point in annealed b.c.c. metals, and the observed absence of this phenomenon in prestrained material. Furthermore, comparison of Figures 7a and 7b illustrates that the predicted influence of m on the stress-strain curve is verified by experiment for those materials where m has been measured.

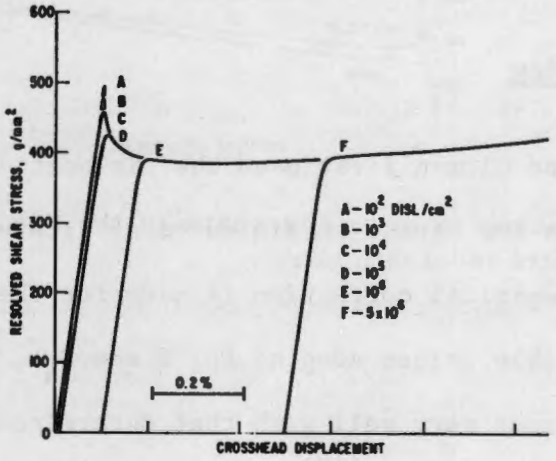

FIGURE 6. EFFECT OF ρ_o' ON THE SHAPE OF THE CALCULATED STRESS-STRAIN CURVE, ALL OTHER PARAMETERS IN EQUATION (9) BEING CONSTANT

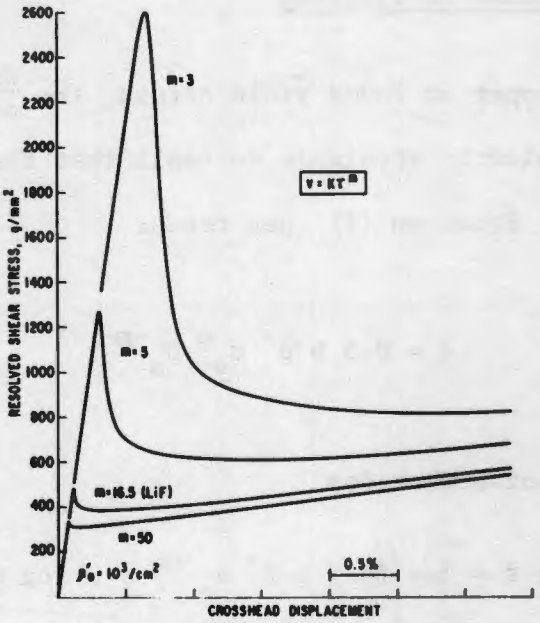

a. Effect of m on the shape of the calculated stress-strain curve

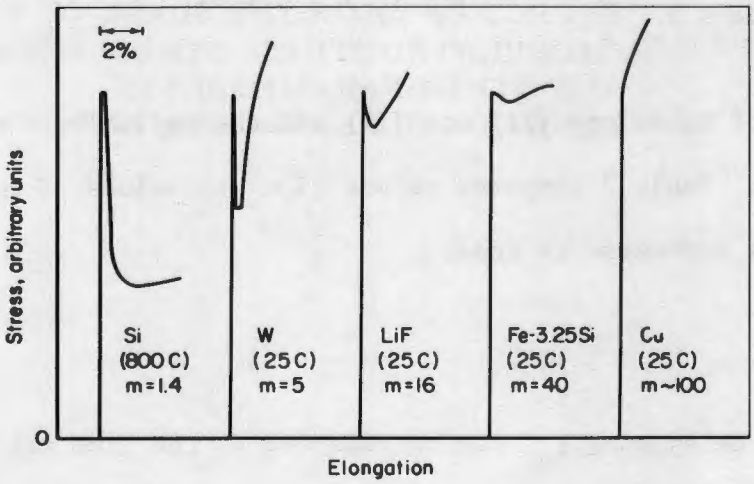

b. Experimental stress-strain curves for materials where values of m are known

FIGURE 7

Strain Rate Dependence of Yielding

At the upper or lower yield stress, the $\frac{d\sigma}{dt}$ term of Equation (9) is zero, and the plastic strain is so small that the work hardening term can be neglected. Equation (9) then reads:

$$\dot{\epsilon} = 0.5\ b\ \rho'\ \sigma_y^{\ m}\ \sigma_o^{\ -m} \tag{10}$$

Taking logarithms of both sides

$$\log \dot{\epsilon} = \log\ (0.5\ b\ \rho'\ \sigma_o^{\ -m}) + m \log \sigma_y$$

or

$$\log \dot{\epsilon} = m \log \sigma_y + \text{CONSTANT} \tag{11}$$

This may be compared to the long established empirical equation describing the strain rate dependence of the yield stress:

$$\log \dot{\epsilon} = m' \log \sigma_y + \text{CONSTANT} \tag{12}$$

A comparison of Equations (11) and (12) affords an indirect method of determining m. Table 3 compares values of m' to values of m determined directly. The agreement is good.

Delay Time

The delay time, t_d, can be regarded as the time taken for a material under constant stress to deform to the minimum detectable strain, say ϵ'. Under these conditions $d\sigma/dt = 0$ and Equation (9) can

TABLE 3. COMPARISON OF THE DIRECT AND INDIRECT METHODS OF DETERMINING m

		m	m′	m″	m‴
LiF	(S)	14.5[1]	14.5[20]		
Fe-Si	(S)	40 ± 5[2]	45[21]		
	(P)		48[21]		
W	(P)		7[32]		
W	(S)	5[6]			
Mo			14[23]	10-15[24]	14[23]
Steel	$\dot{\varepsilon} < 1$		20-50[25,26]		30[27,28]
	$\dot{\varepsilon} > 1$		10-15[29]	10-15[29]	
Cu			~200[30]		
Ag			~300[31]		

S = SINGLE CRYSTAL

P = POLYCRYSTALS

$$m = \frac{d \ln \bar{v}}{d \ln \sigma}$$

$$m' = \frac{d \ln \dot{\varepsilon}}{d \ln \sigma}$$

$$m'' = \frac{d \ln t_d}{d \ln \sigma}$$

$$m''' = \frac{d \ln u}{d \ln \sigma}$$

be rewritten:

$$\int_{\epsilon_p = 0}^{\epsilon'} \frac{d\epsilon_p}{0.5\ b\ (\rho_o' + fC\epsilon_p)\ (\sigma_o)^{-m}\ (\sigma)^m} = \int_0^{t_d} dt \qquad (13)$$

This may be evaluated:

$$\frac{2fC}{b} \left(\frac{\sigma_o}{\sigma}\right)^m \ln\left(1 + \frac{fC\epsilon'}{\rho_o'}\right) = t_d \qquad (14)$$

The delay time may thus be calculated as a function of stress. Figure 8 shows the results of such a calculation, performed using constants appropriate for steel, compared to experimental determinations.

From Equation (14) we may write:

$$\log\left\{\frac{2fC}{b}\ \sigma_o^{\,m} \ln\left(1 + \frac{fC\epsilon'}{\rho_o'}\right)\right\} - m \log \sigma = \log t_d \qquad (15)$$

or since the first term is constant,

$$m = \left[-\frac{d \log t_d}{d \log \sigma} \equiv m''\right] \qquad (16)$$

The term on the right (called m'') represents another indirect method of determining m. In Table 3, a comparison is made of m, m' and m'' for instances where this is possible, and the agreement is encouraging.

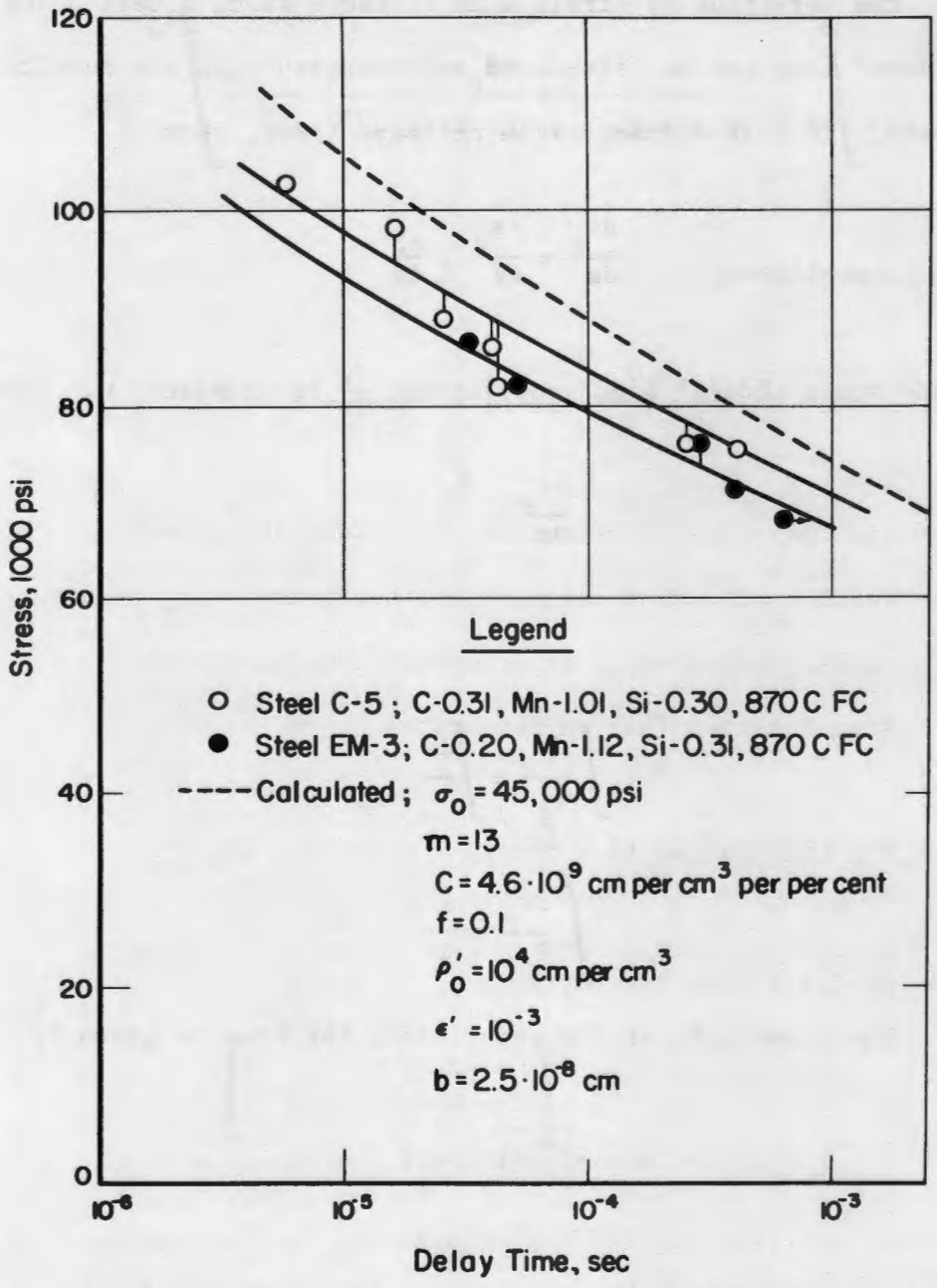

(37)

FIGURE 8. COMPARISON OF EXPERIMENTAL AND CALCULATED VALUES OF DELAY TIME FOR MILD STEEL

Lüders' Bands

The variation of strain with distance along a test piece exhibiting a Lüders' band can be calculated and compared with the results of experiments. If x is distance from the band front, then

$$\frac{d\epsilon_p}{dx} = \frac{d\epsilon_p}{dt} \cdot \frac{dt}{dx} \tag{17}$$

For steady state Lüders' band propagation, $\frac{dx}{dt}$ is constant, u. Thus,

$$\frac{d\epsilon_p}{dx} = \frac{\dot{\epsilon}_p}{u} \tag{18}$$

Thus,

$$\int \frac{d\epsilon_p}{\dot{\epsilon}_p} = \int \frac{dx}{u} \tag{19}$$

and

$$\int \frac{d\epsilon_p}{\dot{\epsilon}_p} = \frac{x}{u} \tag{20}$$

The stress, σ, at any point along the band is given by

$$\sigma = \sigma'_{LY} (1 + \epsilon_p) \tag{21}$$

where σ'_{LY} is the load on the specimen at the lower yield point divided by the initial cross section.

Substituting in Equation (20) values of $\dot{\epsilon}$ from Equation (9)

and the value of σ from Equation (21), we obtain:

$$\frac{x}{u} = \int \frac{d\epsilon_p}{.5\, b\, (\rho_o' + f C \epsilon_p)\, (\sigma_o)^{-m} \{\sigma'_{LY}\, (1 + \epsilon_p) - q\, \epsilon_p\}^m} \qquad (22)$$

since at the lower yield point $d\sigma/dt = 0$. By graphical integration we can solve this equation and thus calculate the variation of strain with distance--that is, the strain profile of the Lüders' band. There is good qualitative agreement with experiment, as is shown in Figure 9.

There remains another indirect method of determining m. This is based on the postulate that there exists a simple relationship between the velocity of a Lüders' band front and the average velocity of the dislocations at the front. This would be the case if for example the band propagated by the injection of mobile dislocations from the band front into the otherwise undeformed matrix. Let the relationship be

$$u = k\bar{v} \qquad (23)$$
$$= k\, \sigma^m\, \sigma_o^{-m}$$

Therefore,

$$m = \left[\frac{d \log u}{d \log \sigma} \equiv m'''\right] \qquad (24)$$

The term on the right will be called m'''. Figure 10 gives an idea of the usefulness of this relationship: the slopes of the lines represent m' and m''' for steel and molybdenum. The agreement is good, and the numerical values appear in Table 3.

The results of Table 3 are important for two reasons. First,

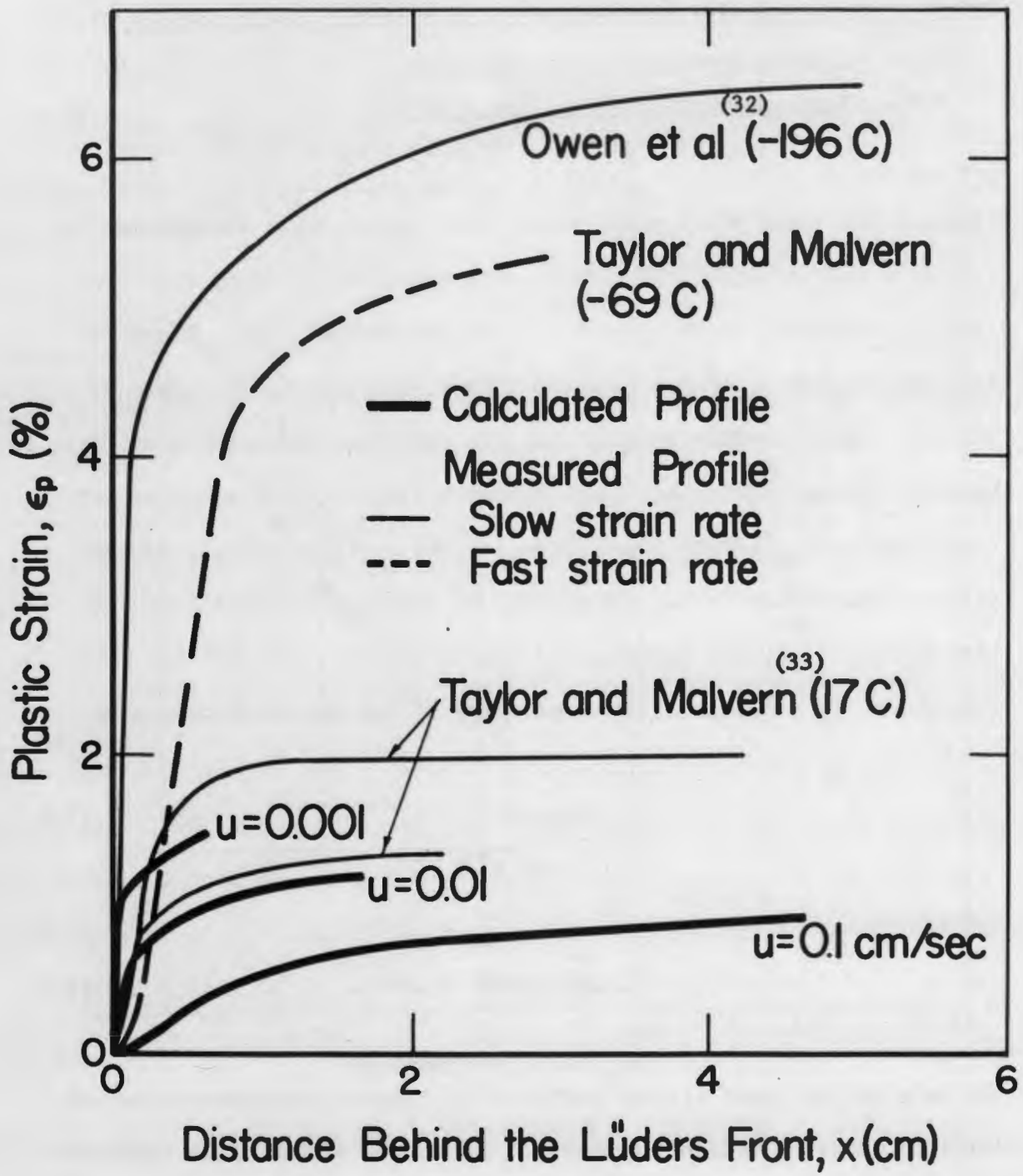

FIGURE 9. RESULTS OF LUDERS' BAND STRAIN PROFILE CALCULATIONS.[7] STRAIN PROFILES PRESCRIBED BY EQUATION (22).

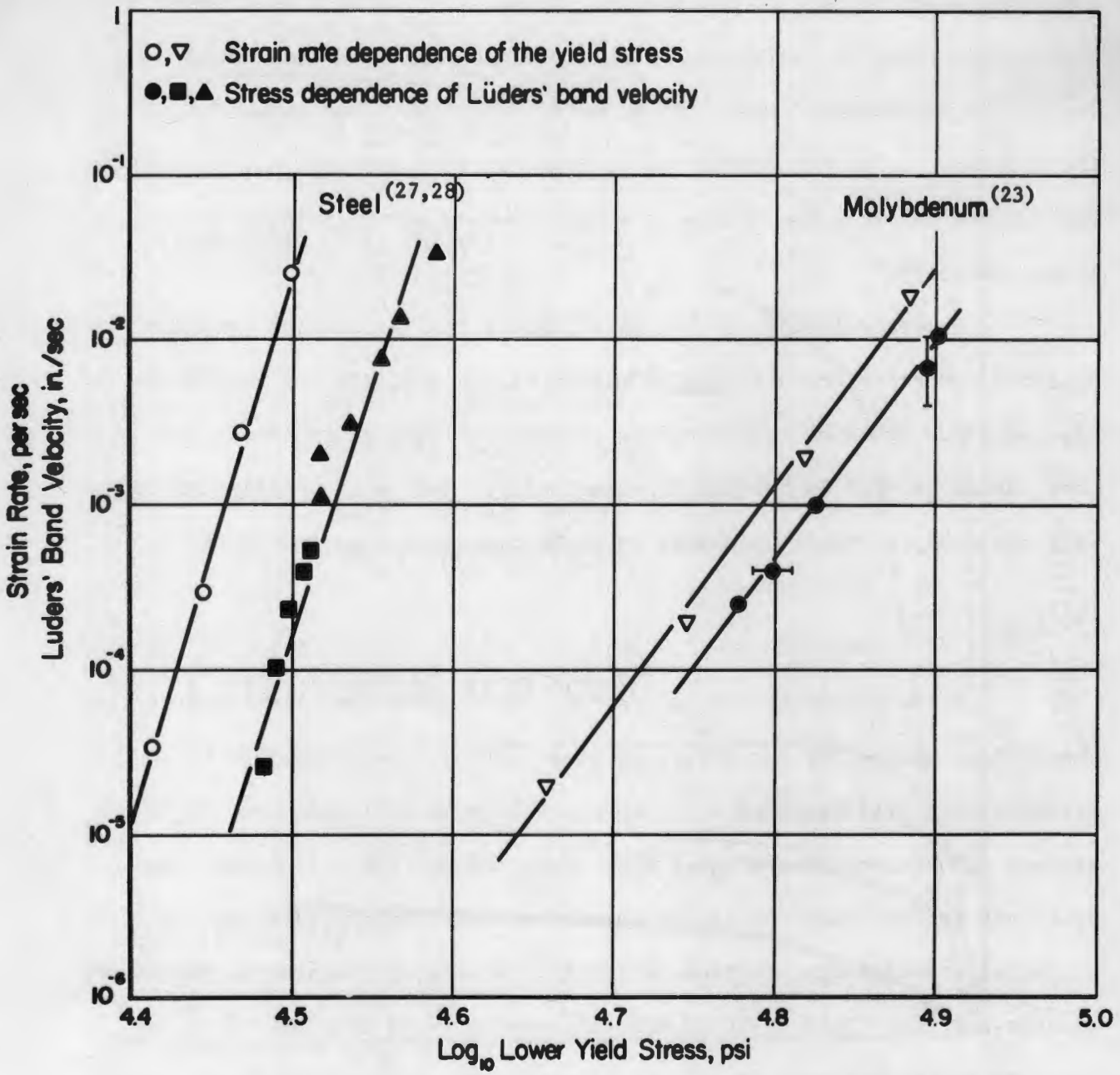

FIGURE 10. A COMPARISON OF m' AND m'''

they lend added support to the theory. Secondly, they show that the stress dependence of dislocation velocity can be inferred indirectly from other measurements which may be more convenient. For example, the values of m for copper and silver have not been measured but it can be inferred from the values of m' that these must be relatively large numbers.

In general then, it can be said that the dislocation dynamics approach describes the yielding of metals very accurately and can therefore be used with some confidence to predict yielding under conditions that cannot be readily handled experimentally. This will be illustrated with one example, namely yielding in the vicinity of a moving crack.

Fracture

It is essential that a treatment of cleavage in plastic materials should take account of the effect of plastic flow. For example, the stresses that will cause an existing crack to grow will also tend to produce deformation at the crack tip. Such deformation will blunt the crack and redistribute the stress thereby making inappropriate the classical stress field solution of Inglis.[34] An adequate approach, therefore, demands a stress field solution that is responsive to deformation at the crack tip. Furthermore, it is necessary that the kinetics of this deformation be known, together with the fracture strength of the material.

Previous attempts at a solution have relied on a modification of the surface energy in order to account for the work done by plastic flow. Unfortunately, this approach ignores the fact that the stress field

of the propagating crack is modified by deformation, and consequently is of limited usefulness.

The model to be described attempts to fulfill all the above requirements and consists of a partially relaxed crack the relaxation of which is described by Dislocation Dynamics.

The model, illustrated in Figure 11, consists of a two-dimensional sharp crack of length 2a, whose tip is surrounded by a circular plastic zone of radius, r. Stresses within this zone are assumed to be substantially relaxed. The extent of the plastic zone is defined as the locus of points where flow begins to occur rapidly, for example where the plastic strain reaches a value of 0.1%. Under these conditions, the crack-plastic zone complex is equivalent to an elliptical hole of semi-major axis, a, and root radius, r. The stress concentration factor, α, in advance of this "hole" can be evaluated from equations derived by Inglis as a function of a/r. The variation of α with distance from the "hole" is illustrated in Figure 12, where it may be seen that the stress gradient close to the elastic-plastic boundary is very steep.

The principle of the calculation is presented in Figure 13, and is directed toward the evaluation of r, and hence α. A crack is assumed to be propagating toward a volume element dV with a velocity U. As the crack approaches, dV experiences a rising stress, (illustrated in the lower diagram) under the influence of which it flows. The condition for the solution of the calculation is that the arrival of the "hole" coincides with the strain in dV reaching a value of 0.1%. Dislocation dynamics provides a unique means of calculating this deformation.

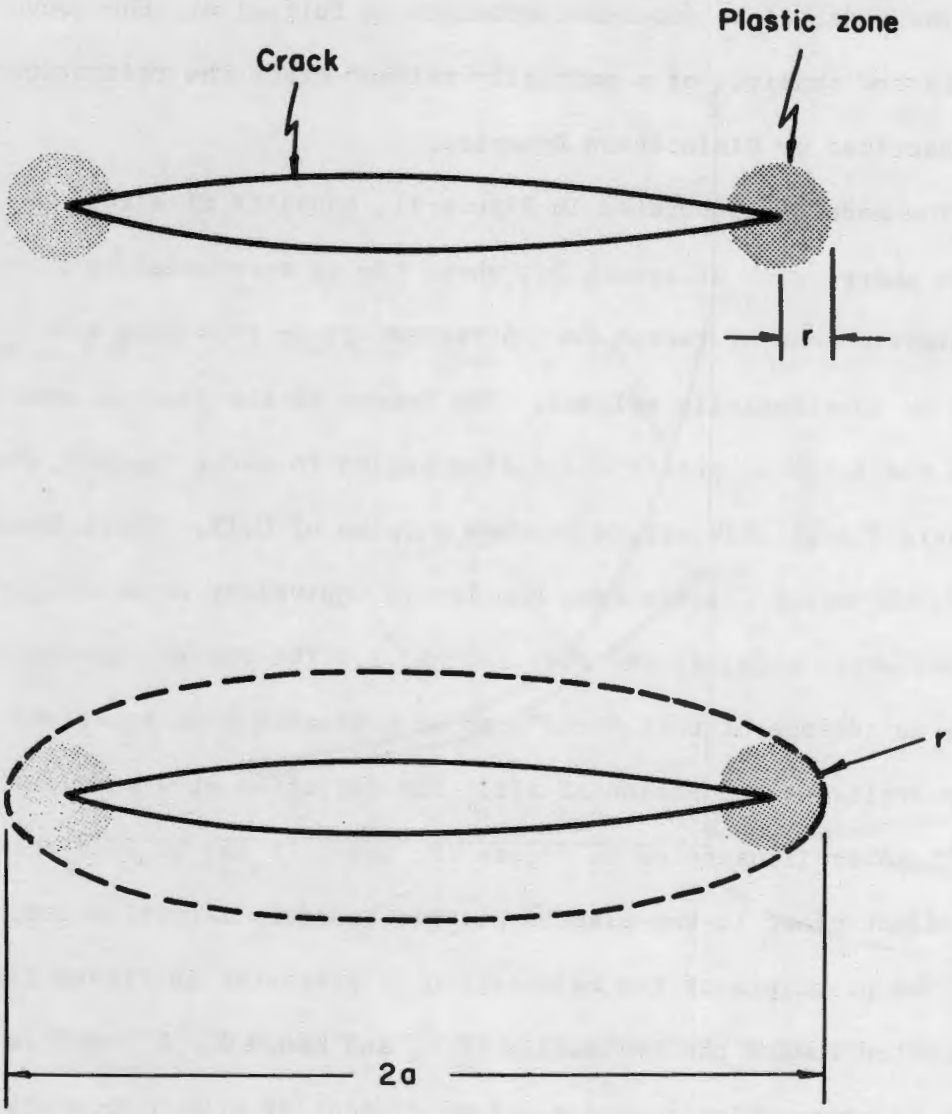

FIGURE 11. THE MODEL OF A PARTIALLY RELAXED BRITTLE CRACK

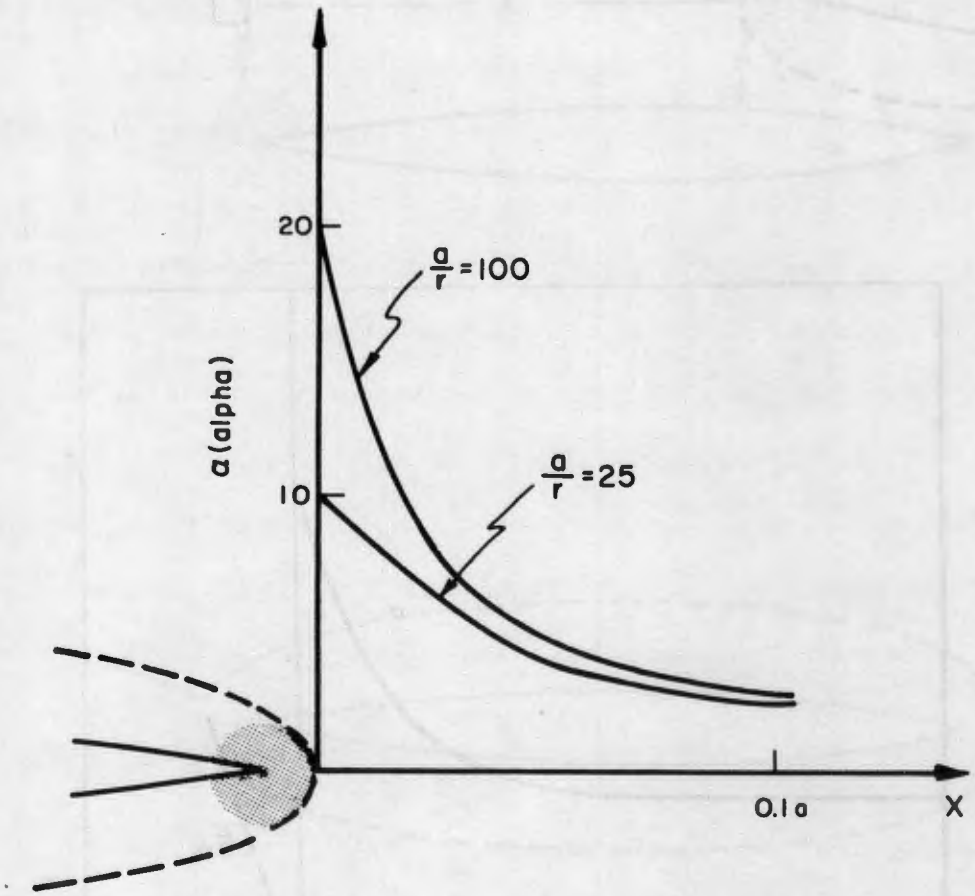

FIGURE 12. CALCULATED STRESS CONCENTRATION OF AN ELLIPTICAL CRACK FOR TWO DIFFERENT VALUES OF a/r

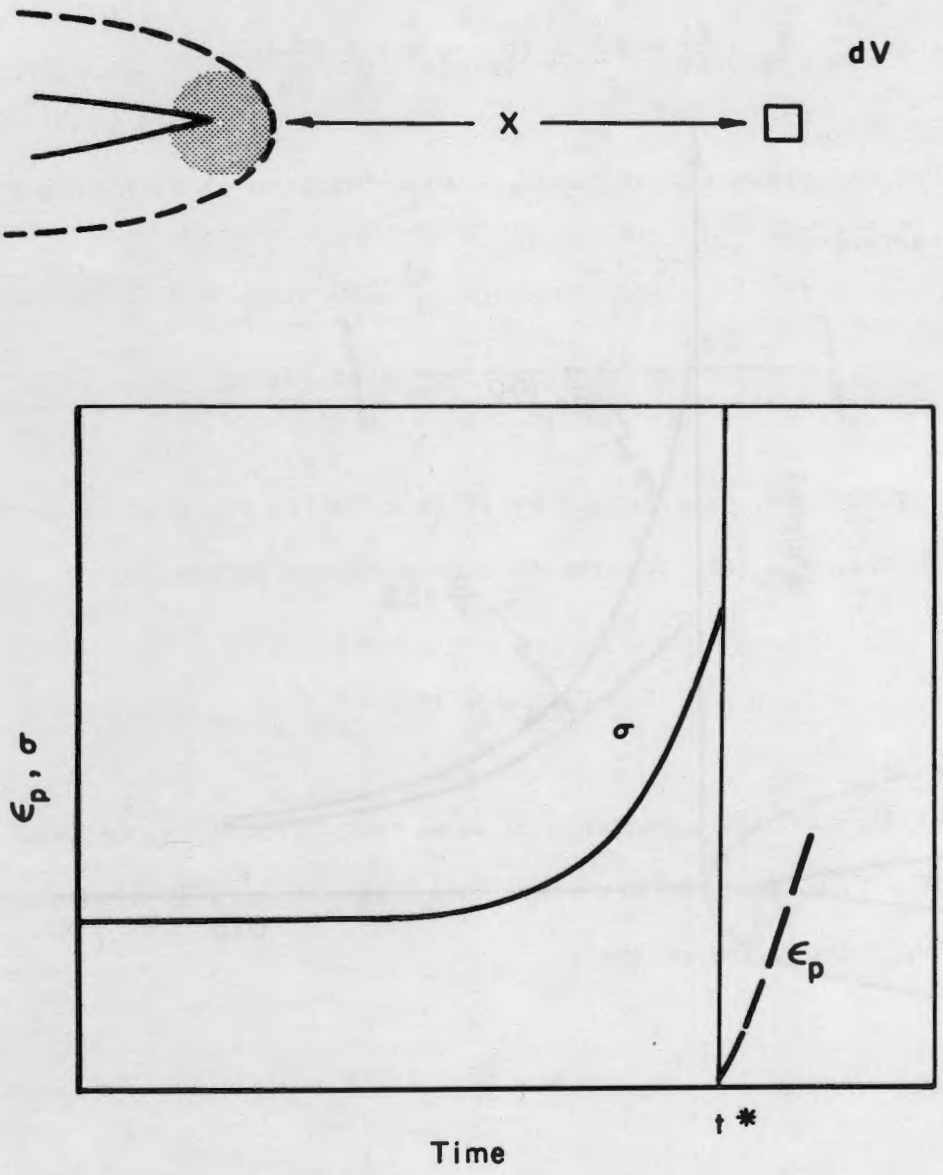

FIGURE 13. SCHEMATIC OF STRESS AND STRAIN AHEAD OF A MOVING CRACK

Recalling Equation (7), the plastic flow of dV may be written:

$$\dot{\epsilon}_p = \frac{d\epsilon}{dt} = 0.5\ b\ (\rho_o' + fC\epsilon_p)\ \left(\frac{\sigma}{\sigma_o}\right)^m \tag{25}$$

Since under the present conditions, σ is a function of t, the equation may be rearranged

$$\int \frac{d\epsilon}{0.5\ b\ (\rho_o' + fC\epsilon_p)\ (\sigma_o)^{-m}} = \int \sigma^m\ dt \tag{26}$$

The local stress, σ, experienced by dV is actually the product of the nominal stress, σ_{NOM}, and the stress concentration factor, α.

$$\sigma = \sigma_{NOM} \cdot \alpha\ (x) \tag{27}$$

where $\alpha(x)$ implies the dependence of α on the distance, x, between dV and the "hole". Since however the crack propagates toward dV with constant velocity U, x and t are related:

$$U = -\frac{dx}{dt} \tag{28}$$

The limits and base of Equation (26) can now be changed from (t) to (x).

$$\int_0^{.001} \frac{d\epsilon}{.5\ b\ (\rho_o' + fC\epsilon_p)\ (\sigma_o)^{-m}} = \frac{(\sigma_{NOM})^m}{U} \int_{x>>a}^{x\ =\ a} [\alpha(x)]^m\ dx \tag{29}$$

Let

$$\frac{(\sigma_{NOM})^m}{U} \int_{x>>a}^{x\ =\ a} [\alpha(x)]^m\ dx = I$$

The left-hand side can be integrated analytically and evaluated for given material parameters. The right-hand side must be integrated numerically and the equality of Equation (29) holds only for one value of a/r (α being a function of a/r). This may be determined by evaluating I for various values of a/r and plotting the graphical relationship between them. The magnitude of a/r corresponding to the left-hand side may then be determined.

The geometry and stress field of the propagating crack are now solved; the solution is sensitive to the values chosen for the parameters, m, U, C and ρ_o'.

In Figure 14, the plastic zone size, r/a, and the maximum stress concentration, α^*, have been determined for various values of m as a function of the crack velocity. The calculations were performed for the case where the applied stress, σ_{NOM} is half the yield stress, σ_y, in a slow tensile test. Consequently, the maximum stress, σ^*, ahead of the crack may be expressed in terms of σ_y. It can be seen that as the crack velocity increases and the time available for plastic relaxation decreases, the plastic zone size becomes progressively smaller. Effectively the crack is blunted to a lesser extent, and consequently higher stresses are generated at the crack tip. The calculation was made for different values of m. The value, m = 5, is characteristic of tungsten. It can be seen that for a fast moving crack in tungsten, stresses of the order of 100 times the yield stress are generated, which approaches plausible values for the theoretical strength. It would therefore be expected that in this material crack propagation by cleavage could occur readily. On the other hand, the stresses generated in materials characterized by higher values of m are much lower. It is, therefore, understandable that f.c.c.

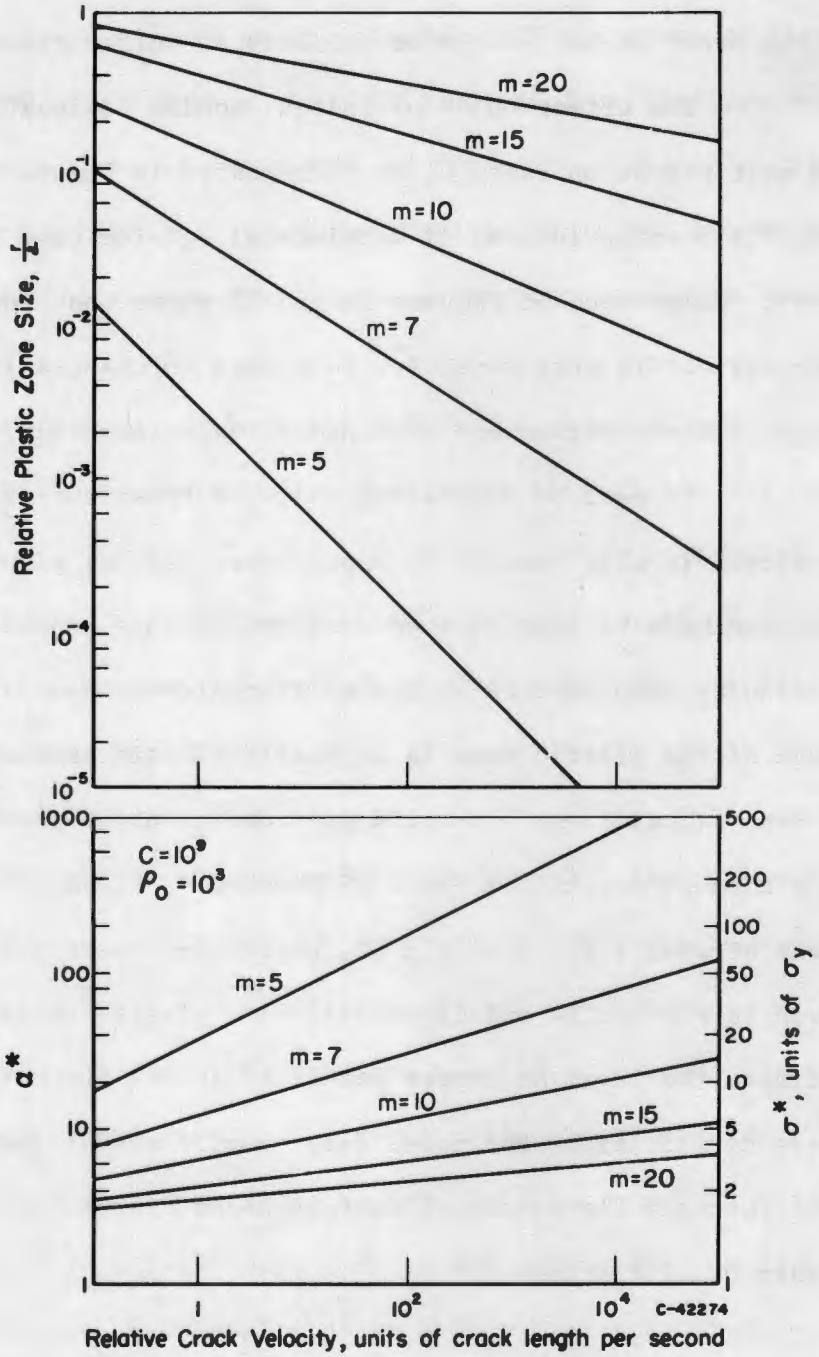

FIGURE 14. EFFECT OF m AND CRACK VELOCITY ON PLASTIC ZONE SIZE AND MAXIMUM STRESS CONCENTRATION FACTOR.

materials, such as copper or silver, that are characterized by m values of the order of 100, would be unlikely to suffer cleavage fracture.

The effect on σ^* of initial mobile dislocation density, ρ_o', and multiplication rate, C, is illustrated in Figure 15. It is apparent that dislocation locking is detrimental, giving rise to larger values of σ^*. Comparison of Figures 14 and 15 shows that for a given crack velocity, σ^* is more sensitive to m than to changes in C and ρ_o' over the range of these parameters encountered experimentally.

It must be emphasized that the treatment of crack propagation developed in this section is approximate and not rigorous. No attempt has been made to take into account constraints imposed on yielding by continuity requirements at the elastic-plastic boundary. The postulated shape of the plastic zone is in itself a basic assumption. Finally, the present calculations are valid for conditions of plane stress: the case of a through-crack in a sheet of thickness, t, when $r \gg t$, but not for plane strain, i.e., $r \ll t$. It, therefore, seems likely that the results given in Figures 14 and 15 overestimate plastic relaxation and underestimate the level of stress generated at the crack tip. In spite of these difficulties, the model does provide useful insights and serves to illustrate the potential usefulness of dislocation dynamics in the treatment of fracture.

CONCLUSIONS

1. A review has been made of current knowledge concerning dislocation multiplication and mobility. Observations are summarized of the

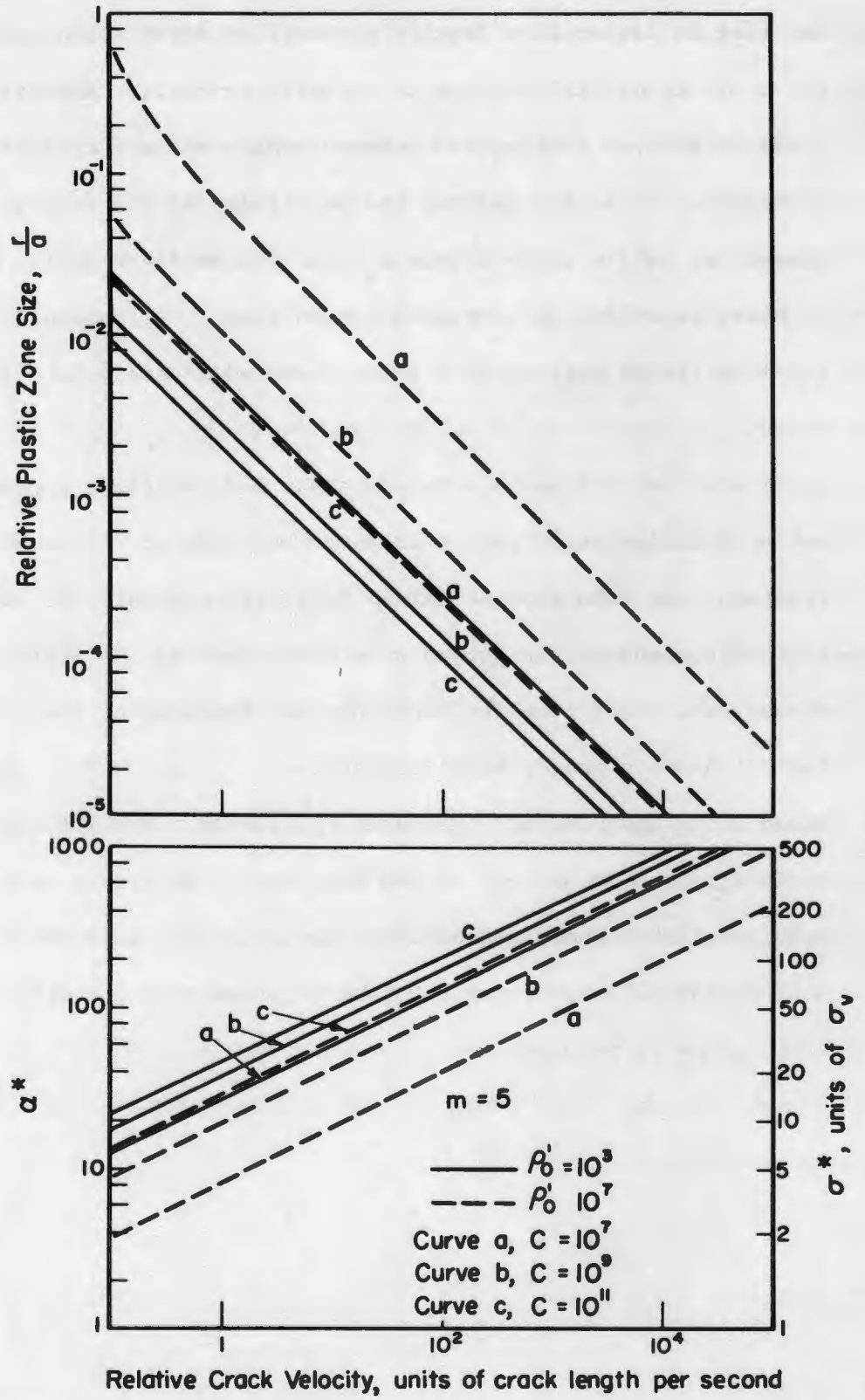

FIGURE 15. EFFECT OF MULTIPLICATION RATE AND INITIAL MOBILE DISLOCATION DENSITY ON PLASTIC ZONE SIZE AND MAXIMUM STRESS CONCENTRATION FACTOR.

increase in dislocation density produced by deformation, and the mobility of dislocations in annealed crystals. Experiments do not yet distinguish between mobile and arrested dislocations. As a consequence, the magnitudes of the initial density of mobile dislocations ρ_o and the mobile fraction f of those generated by straining are in doubt. Furthermore, the mobility of dislocations in cold-worked crystals is not known.

2. Application of Dislocation Dynamics has made possible a quantitative description of the yield point phenomenon. Although the treatment has been applied mainly to single crystals, it satisfactorily predicts the strain rate dependence of the yield stress, the delay time for yielding, and features of the Lüders' band in polycrystalline metals.

3. Dislocation Dynamics has been used to calculate the influence of deformation parameters on the response of materials to a running crack. These calculations indicate that m is the most influential material parameter, small values of m favoring cleavage crack propagation.

REFERENCES

1. Johnston, W. G., and Gilman, J. J., J. App. Phys., 30, p. 129 (1959).
2. Stein, D. F., and Low, J. R., J. App. Phys., 31, p. 362 (1960).
3. Erickson, J. S., J. App. Phys., 33, p. 2499 (1962).
4. Chaudhuri, A. R., Patel, J. R., and Rubin, L. G., J. App. Phys., 33, p. 2736 (1962).
5. Dew-Hughes, D., I.B.M. Journal, 5, p. 279 (1961).
6. Schadler, H. W., and Low, J. R., Final Report on Contract No. Nonr-2614(00) (April, 1962).
7. Hahn, G. T., Acta Met., 10, p. 727 (1962).
8. Keh, A. S., and Weissman, S., Conference on the Impact of Transmission Electron Microscopy on Theories of the Strength of Crystals, Berkeley (to be published by Interscience Publishers, New York) (1961).
9. Patel, J. R., and Alexander, B. H., Acta Met., 4, p. 385 (1956).
10. Hordon, M. J., Acta Met., 10, p. 999 (1962).
11. Livingston, J. D., Acta Met., 10, p. 229 (1962).
12. Young, F. W., J. App. Phys., 33, p. 963 (1962).
13. Van Torne, L. I., L.R.L. Report, University of California, Contract No. W-7405 eng 48 (August, 1962).
14. Owen, W. S., et al., WADD TR 61-181, Part II, p. 236 (October, 1962).
15. Benson, R., Thomas, G., and Washburn, J., "Direct Observations of Imperfections in Crystals", Wiley, p. 375 (1962).
16. Present authors, unpublished work.
17. Cottrell, A. H., "Dislocations and Plastic Flow in Crystals", O.U.P., p. 18 (1948).
18. Conrad, H., Acta Met., 11, p. 75 (1963).
19. Johnston, W. G., J. App. Phys., 33, p. 2716 (1962).

20. Johnston, W. G., Private communications.

21. Stein, D. F., Private communications.

22. Bechtold, J. H., Trans. AIME, 206, p. 142 (1956).

23. Present authors, Unpublished work.

24. Hendrickson, J. A., Wood, D. S., and Clark, D. S., Trans ASM, 48, p. 540 (1956).

25. Winlock, J., Trans. AIME, 197, p. 797 (1953).

26. Manjoine, M. J., Trans. ASME, 66, p. A-211 (1944).

27. Fisher, J. C., and Rogers, H. C., Acta Met., 4, p. 180 (1956).

28. Sylwestrowicz, W., and Hall, E. O., Proc. Phys. Soc., B64, p. 495 (1951).

29. Krafft, J. M., and Sullivan, A. M., Trans. ASM, 51, p. 643 (1959).

30. Carreker, R. P., and Hibbard, W. R., Acta Met., 1, p. 654 (1953).

31. Carreker, R. P., Trans. AIME, 209, p. 112 (1957).

32. Owen, W. S., Averbach, B. L., and Cohen, M., Trans. ASM, 50, p. 634 (1958).

33. Taylor, D. B. C., and Malvern, L. E., Response of Metals to High Velocity Deformation, p. 77, Interscience Publishers, New York (1961).

34. Inglis, C. E., Trans. Inst. Naval Arch., 55, Pt. 1, p. 219 (1913).

35. Gilman, J. J., and Johnston, W. G., J. App. Phys., 31, p. 687 (1960).

36. Present authors, Unpublished work.

37. Krafft, J. M., and Sullivan, A. M., Report to Ship Structure Committee SSC-139, "On the Effects of Carbon and Manganese Content and of Grain Size on Dynamic Strength Properties of Mild Steel".